Domain 5 of the Cation-Independent Mannose 6-Phosphate Receptor Preferentially Binds Phosphodiesters (Mannose 6-Phosphate *N*-Acetylglucosamine Ester)†

Carrie A. Chavez,‡,§ Richard N. Bohnsack,‡,§ Mariko Kudo,|| Russell R. Gotschall,|| William M. Canfield,|| and Nancy M. Dahms*,‡

Department of Biochemistry, Medical College of Wisconsin, Milwaukee, Wisconsin 53226, and Genzyme Corporation, Oklahoma City, Oklahoma 73104

Received June 14, 2007; Revised Manuscript Received August 20, 2007

ABSTRACT: The 300 kDa cation-independent mannose 6-phosphate receptor (CI-MPR) and the 46 kDa cation-dependent MPR (CD-MPR) are key components of the lysosomal enzyme targeting system that bind newly synthesized mannose 6-phosphate (Man-6-P)-containing acid hydrolases and divert them from the secretory pathway. Previous studies have mapped two high-affinity Man-6-P binding sites of the CI-MPR to domains 1−3 and 9 and one low-affinity site to domain 5 within its 15-domain extracytoplasmic region. A structure-based sequence alignment predicts that domain 5 contains the four conserved residues (Gln, Arg, Glu, Tyr) identified as essential for Man-6-P binding by the CD-MPR and domains 1−3 and 9 of the CI-MPR. Here we show by surface plasmon resonance (SPR) analyses of constructs containing single amino acid substitutions that these conserved residues (Gln-644, Arg-687, Glu-709, Tyr-714) are critical for carbohydrate recognition by domain 5. Furthermore, the *N*-glycosylation site at position 711 of domain 5, which is predicted to be located near the binding pocket, has no influence on the carbohydrate binding affinity. Endogenous ligands for the MPRs that contain solely phosphomonoesters (Man-6-P) or phosphodiesters (mannose 6-phosphate *N*-acetylglucosamine ester, Man-P-GlcNAc) were generated by treating the lysosomal enzyme acid α-glucosidase (GAA) with recombinant GlcNAc-phosphotransferase and uncovering enzyme (*N*-acetylglucosamine-1-phosphodiester α-*N*-acetylglucosaminidase). SPR analyses using these modified GAAs demonstrate that, unlike the CD-MPR or domain 9 of the CI-MPR, domain 5 exhibits a 14−18-fold higher affinity for Man-P-GlcNAc than Man-6-P, implicating this region of the receptor in targeting phosphodiester-containing lysosomal enzymes to the lysosome.

Lysosomes require a repertoire of over 50 different acid hydrolases to carry out the degradative metabolism of proteins and other macromolecules. Targeting of newly synthesized acid hydrolases to lysosomes is dependent upon specific recognition in the *trans* Golgi network (TGN)[1] of mannose 6-phosphate (Man-6-P) residues on their N-linked oligosaccharides by two members of the P-type lectin family, the 300 kDa cation-independent mannose 6-phosphate receptor (CI-MPR) and the 46 kDa cation-dependent MPR (CD-MPR) (*1*−*3*). The post-translational modification of lysosomal enzymes with Man-6-P occurs by a two-step process (Figure 1A). The first enzyme, UDP-*N*-acetylglucosamine: lysosomal enzyme *N*-acetylglucosamine-1-phosphotransferase (GlcNAc-phosphotransferase; IUBMB accession number EC 2.7.8.17), acts in early Golgi compartments and attaches *N*-acetylglucosamine (GlcNAc)-1-phosphate to the C-6 hydroxyl group of one or more mannose residues to form a phosphodiester, mannose 6-phosphate *N*-acetylglucosamine ester (Man-P-GlcNAc) (Figure 1A,B) (*4*−*7*). The second enzyme, *N*-acetylglucosamine-1-phosphodiester α-*N*-acetylglucosaminidase, which is often referred to as the "uncovering enzyme" (IUBMB accession number EC 3.1.4.45), removes the GlcNAc moiety in the TGN to generate a phosphomonoester (Figure 1A,C) (*8*−*12*). The MPRs transport their cargo from the TGN to endosomal compartments where the acidic environment of the endosome facilitates the dissociation of the enzyme−receptor complex. The lysosomal enzymes become packaged into lysosomes, while the MPRs recycle back to the TGN to repeat the process.

The MPRs are type I transmembrane glycoproteins. The large extracytoplasmic region of the CI-MPR is composed of 15 contiguous domains (Figure 2A) that display similar sizes (∼150 residues) and cysteine distributions and exhibit significant amino acid identity (14−38%) when compared to each other and to the ∼160-residue extracytoplasmic region of the CD-MPR (*13*). Unlike the homodimeric CD-MPR, which contains one Man-6-P binding site per polypep-

† This work was supported by National Institutes of Health Grant R01DK42667 (N.M.D.).

* To whom correspondence should be addressed. Phone: (414) 456-4698. Fax: (414) 456-6510. E-mail: ndahms@mcw.edu.

‡ Medical College of Wisconsin.

§ These authors contributed equally to this work.

|| Genzyme Corp.

[1] Abbreviations: TGN, *trans* Golgi network; Man-6-P, mannose 6-phosphate; CI-MPR, cation-independent mannose 6-phosphate receptor; CD-MPR, cation-dependent mannose 6-phosphate receptor; GlcNAc-phosphotransferase, UDP-*N*-acetylglucosamine:lysosomal enzyme *N*-acetylglucosamine-1-phosphotransferase; Man-P-GlcNAc, mannose 6-phosphate *N*-acetylglucosamine ester; uncovering enzyme, *N*-acetylglucosamine-1-phosphodiester α-*N*-acetylglucosaminidase; Man-P-OCH_3, mannose 6-phosphate methyl ester; SPR, surface plasmon resonance; GAA, acid α-glucosidase; Ni−NTA, nickel−nitrilotriacetic acid; ConA, concanavalin A; *endo* H, *endo*-β-*N*-acetylglucosaminidase H; HM-GAA, acid α-glucosidase with high-mannose-type glycans; spPAP, sweet potato purple acid phosphatase; HPAEC, high-performance anion exchange chromatography; PNGase F, peptide *N*-glycosidase F; Glc-6-P, glucose 6-phosphate.

10.1021/bi7011806 CCC: $37.00
Published on Web 10/10/2007

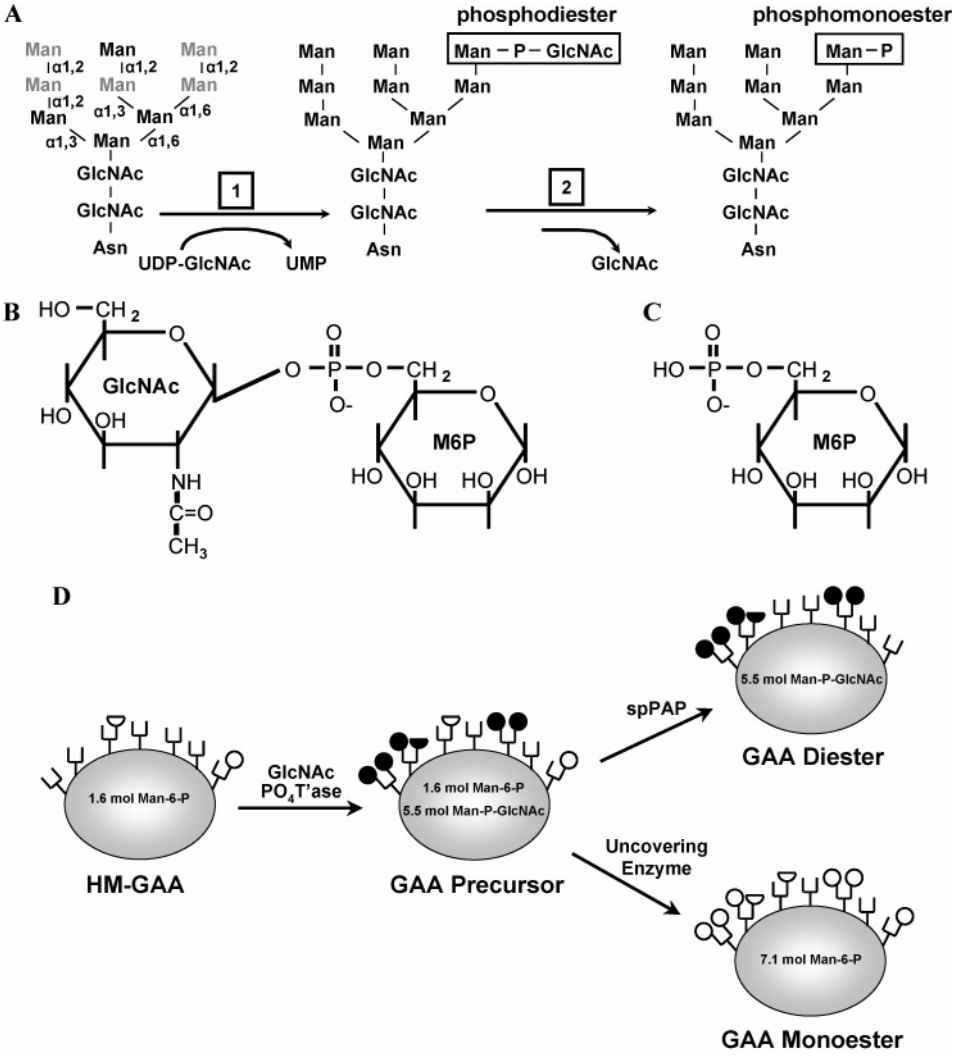

FIGURE 1: Modification of *N*-glycans on lysosomal enzymes. (A) Phosphorylation of mannose residues on N-linked oligosaccharides occurs in two steps. First, the GlcNAc-phosphotransferase transfers GlcNAc-1-phosphate from UDP-GlcNAc to the C-6 hydroxyl group of mannose to form a Man-P-GlcNAc phosphodiester. Second, the uncovering enzyme removes the GlcNAc moiety, exposing the Man-6-P phosphomonoester. The five potential sites of mannose phosphorylation are indicated in gray. (B) Structure of Man-P-GlcNAc phosphodiester. (C) Structure of Man-6-P phosphomonoester. (D) Recombinant human GAA isolated from kifunensine-treated CHO-K1 cells (HM-GAA) contains seven N-linked oligosaccharides (two-pronged fork symbol) and 1.6 mol of the phosphomonoester Man-6-P/mol of GAA (empty circle, empty half-circle). HM-GAA was incubated with GlcNAc-phosphotransferase (GlcNAc PO_4T'ase), resulting in the addition of 5.5 mol of the GlcNAc phosphodiester Man-P-GlcNAc/mol of GAA (filled circle, filled half-circle). The resulting GAA precursor was subjected to incubation with either spPAP, which removes the phosphate group from phosphomonoesters, or uncovering enzyme, which removes the GlcNAc moiety, to generate the GAA diester and GAA monoester, respectively.

tide (*14*), the CI-MPR contains three distinct carbohydrate binding sites: two high-affinity sites map to domains 1−3 and 9 (*15*, *16*), with essential residues for carbohydrate recognition residing in domains 3 and 9 (*17*), and a recently identified low-affinity site has been localized to domain 5 (*18*). In contrast to their similar affinities for Man-6-P (K_i = 18 and 23 μM, respectively), domains 1−3 and 9 of the CI-MPR exhibit differences in their binding properties to various mannose-containing glycans (*16*, *19*). Although domain 5 has been shown to have an approximately 300-fold lower affinity for Man-6-P than domains 1−3 and 9 (*18*), its carbohydrate binding specificity has not been determined.

To date, the structures of two out of the four Man-6-P binding sites of the MPRs have been determined: the crystal structure of the extracytoplasmic region of the CD-MPR (*20*, *21*) and domains 1−3 of the CI-MPR in complex with Man-6-P (*22*) revealed the residues that are within hydrogen-bonding distance to the carbohydrate and demonstrated that domains 1−3 of the CI-MPR exhibit similar folds which are also similar to that of the extracytoplasmic region of the CD-MPR. The structures show that four residues (Gln, Arg, Glu, Tyr) contact the 2-, 3-, and 4-hydroxyl groups of the mannose ring. These residues are conserved in the CD-MPR and domains 3, 5, and 9 of the CI-MPR (Figure 2B), and mutagenesis studies have confirmed their critical role in carbohydrate recognition by the CD-MPR and domains 3 and 9 of the CI-MPR (*17*, *23*, *24*). However, the role of these conserved residues (Gln, Arg, Glu, Tyr) in carbohydrate recognition by domain 5 is not known.

In the current study, site-directed mutagenesis and surface plasmon resonance (SPR) analyses were performed to probe the architecture and ligand specificity of the carbohydrate binding pocket contained within domain 5 of the CI-MPR. Domain 5 mutants containing single amino acid substitutions were generated to evaluate the role of the conserved Gln-

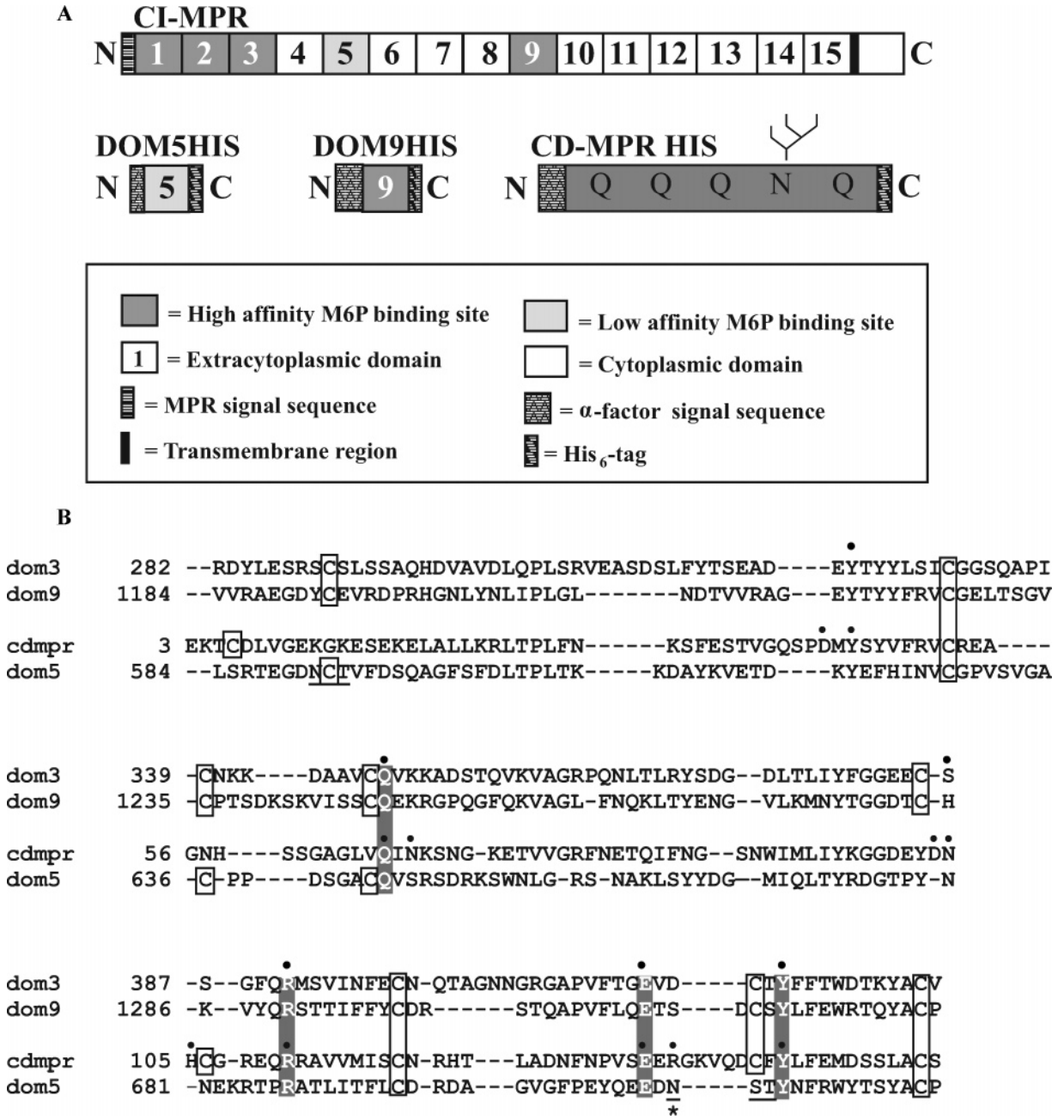

FIGURE 2: Man-6-P binding sites of the CI-MPR and CD-MPR. (A) Schematic diagram of the full-length CI-MPR (top), truncated CI-MPR constructs Dom5His and Dom9His, and truncated CD-MPR construct CD-MPRHis (bottom). The MPRs are type I integral membrane proteins, each with an N-terminal signal sequence, an extracytoplasmic region, a single transmembrane region, and a C-terminal cytoplasmic domain. The CI-MPR has a large extracytoplasmic region comprised of 15 contiguous domains, each ~150 residues in length. The Dom5His and Dom9His constructs contain a substituted N-terminal yeast signal sequence plus a C-terminal tag of six histidine residues. The glycosylation-deficient, truncated CD-MPR construct contains a substituted N-terminal yeast signal sequence, 154 residues of the 159-residue extracytoplasmic region, and 6 histidine residues at the C-terminus. Only one out of the five *N*-glycosylation sites (N) is retained (at position 81), with glutamine (Q) substitutions placed at positions 31, 57, 68, and 87. (B) Structure-based sequence alignment of domains 3 (dom3), 9 (dom9), and 5 (dom5) of the bovine CI-MPR and the extracellular region of the bovine CD-MPR (cdmpr). Residues that are within hydrogen-bonding distance of Man-6-P, as determined by the crystal structure of the CD-MPR (PDB ID 1C39) and domains 1−3 of the CI-MPR (PDB ID 1SZO), are indicated with a closed circle above the sequence. Conserved cysteines are boxed. The four residues essential for carbohydrate binding are shaded. The two *N*-glycosylation sites in domain 5 are underlined, and the star indicates the asparagine residue at position 711 that was mutated to remove the C-terminal *N*-glycosylation site.

644, Arg-687, Glu-709, and Tyr-714 residues and an adjacent *N*-glycosylation site at position 711 in Man-6-P binding. In addition, the generation of a lysosomal enzyme, acid α-glucosidase (GAA), with defined glycans by enzymatic treatment using recombinant GlcNAc-phosphotransferase alone or recombinant GlcNAc-phosphotransferase plus recombinant uncovering enzyme allowed, for the first time, a comparison of the binding properties of the two MPRs with an endogenous ligand that contains solely phosphomonoesters (Man-6-P) or solely phosphodiesters (Man-P-GlcNAc).

EXPERIMENTAL PROCEDURES

Generation of Constructs. The Dom5His construct (residues 584−725 followed by a His_6 tag) in the pGAPZαA expression vector (Invitrogen) was described previously (*18*).

Dom5His constructs containing a single amino acid substitution (Q644E, R687K, E709Q, N711Q, or Y714F) were generated using a single-step polymerase chain reaction-based method using forward and reverse primers (Integrated DNA Technologies, Inc.; the mutagenic codon is underlined): Q644E, forward mutagenic primer 5′-TCC GTG GGC GCC TGC CCG CCG GAC TCG GGG GCC TGT GAA GTG TC-3′, reverse primer 5′-TCGACGGCGCTAT-TCAGATC-3′ located in the vector; R687K, forward mutagenic primer 5′-ATG ATC CAG CTG ACC TAC AGG GAC GGC ACA CCC TAC AAT AAC GAG AAG CGC ACG CCG AAG GCC ACG CTC ATC ACC-3′, reverse primer 5′-ATTCATCAGCTGCGAGATAGGCTGATCAG-GAGCAAGC-3′ located in the vector; E709Q, forward primer located in the vector (pgapαup) 5′-GGATTTCGAT-GTTGCTGTTTTGCC-3′, reverse mutagenic primer 5′-T TGT TCT AGA TCA GTG GTG GTG GTG GTG GTG CGG GCA GGC GTA ACT GGT GTA CCA CCG GAA GTT GTA TGT AGA GTT ATC CTG CTC CTG ATA TTC GGG-3′; Y714F, pgapαup forward primer, reverse mutagenic primer 5′-T TGT TCT AGA TCA GTG GTG GTG GTG GTG GTG CGG GCA GGC GTA ACT GGT GTA CCA CCG GAA GTT GAA TGT AGA GTT ATC-3′. The N711Q mutation, which removed the C-terminal *N*-glycosylation site, was generated using the pgapαup forward primer and the reverse mutagenic primer 5′-T TTT TGT TCT AGA TCA GTG GTG GTG GTG GTG GTG CGG GCA GGC GTA ACT GGT GTA CCA CCG GAA GTT GTA TGT AGA TTG ATC TTC CTC CTG-3′. DNA sequencing (Protein and Nucleic Acid Core Facility, Medical College of Wisconsin) confirmed the presence of each mutation. The Dom9His construct (residues 1184−1327 of the CI-MPR followed by a His_6 tag (*17*)) and the CD-MPRHis construct (residues 1−154 containing only a single *N*-glycosylation site at position 81 plus a C-terminal His_6 tag (*24*)) in the pGAPZαA expression vector were described previously.

Expression and Purification of CI-MPR Constructs. *Pichia pastoris* transformants expressing Dom5His (*18*), Dom9His (*17*), and CD-MPRHis (*24*) were obtained previously. Mutant Dom5His cDNA constructs encoding single amino acid substitutions were linearized with *Bsp*HI and transformed into *P. pastoris* wild-type strain X-33 (Invitrogen) by electroporation, and Zeocin-resistant transformants were selected as described previously (*25*). Positive clones were inoculated in liquid medium (1% yeast extract, 2% peptone, and 2% dextrose), and cultures were harvested after 3 days of growth at 30 °C. Following removal of the cells by centrifugation, the medium was dialyzed against nickel binding buffer (20 mM Tris, 10 mM imidazole, and 500 mM NaCl, pH 8.0). The dialyzed medium was passed over a nickel−nitrilotriacetic acid (Ni−NTA) agarose (Qiagen) column, washed, and then eluted with nickel binding buffer containing 100 mM imidazole (Dom9His, Dom5His, and Dom5His mutants) or 200 mM imidazole (CD-MPRHis). Purified Dom5His and Dom5His mutants were subsequently dialyzed against concanavalin A (ConA) binding buffer (20 mM Tris, pH 7.5, 150 mM NaCl, 1 mM $CaCl_2$, 1 mM $MnCl_2$, and 1 mM $MgCl_2$) and subjected to ConA Sepharose (Sigma) affinity chromatography to separate glycosylated from nonglycosylated species. The glycosylated proteins were eluted from the column with ConA binding buffer containing 0.5 M methyl α-D-mannoside. The glycosylated proteins were then subjected to Ni−NTA agarose affinity chromatography to remove any contaminating ConA. All proteins were extensively dialyzed against MES buffer (50 mM MES, pH 6.5, 150 mM NaCl, 5 mM β-glycerophosphate, and 10 mM $MnCl_2$) and concentrated by filtration using a 4 mL Vivaspin spin column containing a poly(ether sulfone) membrane with a 5 kDa nominal molecular mass limit. The Bradford protein assay (Bio-Rad) with bovine serum albumin as the standard was used to estimate protein yields.

endo-β-N-Acetylglucosaminidase H (endo H) Digestion. Purified Dom5His or N711Q protein was incubated with *endo* H (5 mU, Roche Molecular Biochemicals) in buffer containing 100 mM imidazole, 20 mM Tris, and 500 mM NaCl, pH 6.0, at 37 °C for 16 h. The samples were resolved by SDS−PAGE and detected by silver staining as described by the manufacturer (Bio-Rad).

Purification of Human β-Glucuronidase. Human β-glucuronidase was collected from serum-free conditioned medium from cells which overexpress and secrete this lysosomal enzyme (MTX 3.2 cells were generously provided by Dr. William Sly, St. Louis University School of Medicine, St. Louis, MO). β-Glucuronidase was purified by affinity chromatography on a CI-MPR Affigel-10 column to remove nonphosphorylated enzyme as described previously (*26*).

Generation of Recombinant Human GAA with GlcNAc1-P-6-Man (GAA Diester) and Man-6-P (GAA Monoester). The GAA diester and the GAA monoester were prepared from recombinant human GAA with high-mannose-type glycans (HM-GAA) using recombinant human GlcNAc-phosphotransferase (*27*), uncovering enzyme (*9*), and/or sweet potato purple acid phosphatase (spPAP) (*28*) in vitro (see Figure 1D). HM-GAA was purified from the conditioned medium of CHO-K1 cells stably transfected with recombinant human GAA cDNA (*29*) that were cultured in the presence of the α-mannosidase inhibitor kifunensine (2.5 mg/L; Industrial Research, New Zealand). HM-GAA contains endogenous phosphomonoester (see Figure 5A). The transfer of GlcNAc-1-phosphate to HM-GAA was performed by incubation of 10% (w/w) GlcNAc-phosphotransferase with GAA in buffer (50 mM sodium acetate, pH 6.5, 20 mM $MnCl_2$, and 0.0002% β-mercaptoethanol) containing 3 mM UDP-GlcNAc (Roche) for 72 h at 20 °C under an argon atmosphere. This incubation results in the generation of the GAA precursor (the "GAA precursor" described in this paper refers to a glycosylation intermediate, rather than to the newly synthesized form of GAA which has not undergone proteolytic processing except for removal of the N-terminal signal sequence (*29*)). To prepare the GAA diester, the endogenous phosphate monoester was removed by incubation (48 h) with spPAP (2000 U/mg of GAA) after purification of GAA precursor from GlcNAc-phosphotransferase (see below) and adjustment of the pH to 4.5. To prepare the GAA monoester, the covering GlcNAc was removed from the GAA precursor by incubation (3 h) of 1% (w/w) uncovering enzyme with GAA precursor. After the reaction, GAA precursor and GAA monoester were purified from the other proteins (GlcNAc-phosphotransferase and/or uncovering enzyme) by affinity/size exclusion chromatography on a Superdex 200 (GE healthcare). GAA slows on the Superdex 200 since it has a slight affinity for the dextran backbone of the Superdex 200 matrix. GAA diester was purified from spPAP by cation

exchange chromatography using SP Sepharose XL (GE healthcare) with a KCl gradient in 50 mM sodium acetate, pH 4.5. The carbohydrate composition of the GAA molecules was determined after hydrolysis in 4 N TFA at 100 °C for 4 h followed by high-performance anion exchange chromatography (HPAEC) separation on a CarboPac PA10 (Dionex). Neutral and amino sugars were separated by isocratic elution using 15 mM NaOH. Man-6-P was eluted by a gradient (60−300 mM) of sodium acetate in 100 mM NaOH. *N*-Glycans were released from GAA molecules using peptide *N*-glycosidase F (PNGase F; New England Biolabs) following the manufacturer's instructions and separated on a CarboPac PA100 (Dionex) by a gradient (5−300 mM) of sodium acetate in 100 mM NaOH to determine the number of phosphate molecules.

Synthesis and Purification of [^{3}H]-N-Acetylglucosaminyl 6-Phosphomethylmannoside Diester ([^{3}H]GlcNAc-α-P-Man-α-Me). [^{3}H]GlcNAc-α-P-Man-α-Me was synthesized and purified following the method described by Mullis and Ketcham (*30*) except that recombinant soluble human GlcNAc-phosphotransferase (*27*) was used as the enzyme source instead of a lysate derived from the soil amoeba *Acathamoeba castellanii*. Briefly, the molecule was synthesized from UDP-[^{3}H]GlcNAc and methyl α-D-mannoside (Sigma) using GlcNAc-phosphotransferase and purified by size exclusion chromatography using Sephadex G-25 equilibrated in 7% (v/v) propanol. The concentration of [^{3}H]-GlcNAc-α-P-Man-α-Me was determined by carbohydrate composition analysis.

Biosensor Studies. All SPR measurements were performed at 25 °C using a Biacore 3000 instrument (Biacore, Piscataway, NJ). CM5 research grade sensor chips, surfactant P20, and amine coupling kits were also obtained from Biacore. Purified proteins (β-glucuronidase, GAA phosphomonoester, GAA phosphodiester, GAA phosphodiester precursor, Dom5His, Dom9His) were immobilized on CM5 sensor chips following activation of the surface using 1-ethyl-3-[3-(dimethylamino)propyl]carbodiimide and *N*-hydroxysuccinimide as recommended by the manufacturer. Briefly, the proteins were injected onto the activated dextran surface at a concentration of 10−20 μg/mL in 10 mM sodium acetate buffer, pH 5.0 (except β-glucuronidase and GAA phosphodiester, for which 10 mM sodium acetate buffer, pH 4.5, was used), using immobilization buffer (10 mM MES, pH 6.5, 150 mM NaCl, and 0.005% (v/v) P20) as the running buffer. After coupling, unreacted *N*-hydroxysuccinimide ester groups were blocked with ethanolamine. The reference surface was treated in the same way except that protein was omitted. Samples of purified proteins (Dom5His, Dom5His mutants (Q644E, R687K, E709Q, N711Q, and Y714F), Dom9His, CD-MPRHis, GAA phosphomonoester, GAA phosphodiester) were prepared in running buffer (50 mM MES, pH 6.5, 150 mM NaCl, 10 mM $MnCl_2$, 5 mM β-glycerophosphate, and 0.005% (v/v) P20) and were injected in a volume of 80 μL over the coupled and reference flow cells at a flow rate of 40 μL/min. After 2 min, the solutions containing the purified proteins were replaced with buffer, and the complexes were allowed to dissociate for 2 min. The sensor chip surface was regenerated with a 10 μL injection of 10 mM HCl at a flow rate of 10 μL/min. The surface was allowed to re-equilibrate in running buffer for 1 min prior to subsequent injections. In some experiments, Dom5His (500 nM) or Dom9His (50 nM) was flowed over sensor surfaces immobilized with either GAA monoester or GAA diester in the presence of increasing concentrations of glucose 6-phosphate (Glc-6-P) (Sigma), Man-6-P (Sigma), or *N*-acetylglucosaminyl 6-phosphomethylmannoside diester. The response at equilibrium (R_{eq}) for each concentration of protein was determined by averaging the response over a 10 s period within the steady-state region of the sensorgram using the BIAevaluation software package (version 4.0.1). R_{eq} was plotted versus the concentration of protein and fitted by nonlinear regression to a one-site saturation binding model using the equation $y = (R_{max}[MPR])/(K_d + [MPR])$ (SigmaPlot version 10.0, Systat Software, Inc.). All response data were double-referenced (*31*), where controls for the contribution of the change in refractive index were performed in parallel with flow cells derivatized in the absence of protein and subtracted from all binding sensorgrams.

RESULTS

Site-Directed Mutagenesis of Domain 5 of the CI-MPR. In contrast to the CD-MPR, which contains a single high-affinity Man-6-P binding site, we have recently shown that the CI-MPR contains three different phosphomannosyl binding sites, two high-affinity sites which map to domains 1−3 and 9 and a low-affinity site that is localized to domain 5 (*18*). The crystal structure of the extracytoplasmic region of the CD-MPR (*20*, *21*) and domains 1−3 of the CI-MPR complexed with Man-6-P (*22*) revealed the residues within the binding pocket. The structures show that both the CD-MPR and domain 3 of the CI-MPR exhibit the same fold and similar disulfide bonding (CD-MPR has three out of the four disulfide bonds contained within domain 3 of the CI-MPR) and use identical residues (Gln, Arg, Glu, Tyr) (see Figure 2B) located in virtually the same position in the binding pocket to contact the 2-, 3-, and 4-hydroxyl groups of the mannose ring. A structure-based sequence alignment (Figure 2B) predicts that the other high-affinity binding site located in domain 9 of the CI-MPR will have a three-dimensional structure similar to that of domain 3: domain 9 exhibits a similar disulfide bonding pattern and contains these four conserved residues (Gln, Arg, Glu, Tyr), and mutagenesis studies have confirmed their critical role in carbohydrate recognition by the CD-MPR (*23*, *24*) and domains 3 and 9 of the CI-MPR (*17*). The presence of these four residues in domain 5 at positions equivalent to those found in the three high-affinity binding sites (Figure 2B) suggests that these residues are key determinants for carbohydrate recognition by domain 5. The alignment (Figure 2B) also reveals that domain 5 is missing two cysteines that form a critical disulfide bridge within the binding pocket of the CD-MPR (*20*, *21*) and domain 3 of the CI-MPR (*22*). In place of one of these cysteine residues is a serine residue that comprises an *N*-glycosylation site at position 711, which raises the possibility that the presence of an *N*-glycan could affect the ability of domain 5 to bind Man-6-P. To test these hypotheses, site-directed mutagenesis was performed to generate single amino acid substitutions in the Dom5His cDNA construct. Conservative substitutions were selected that would significantly perturb hydrogen-bonding potential to Man-6-P (Q644E, R687K, E709Q, or Y714F) or eliminate the *N*-glycan at position 711 (N711Q).

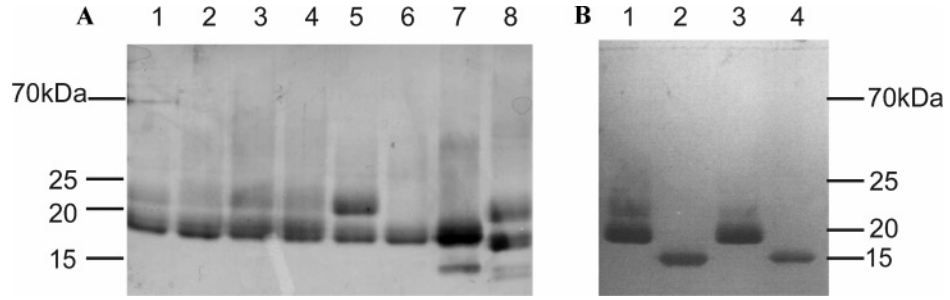

FIGURE 3: Purification and glycosylation status of Dom5His constructs. (A) Following Ni−NTA and ConA affinity chromatography, the purified MPR constructs (3 μg) were resolved on a 12% nonreducing SDS−polyacrylamide gel and visualized by silver staining: lane 1, wild-type Dom5His; lane 2, Y714F; lane 3, R687K; lane 4, Q644E; lane 5, E709Q; lane 6, N711Q; lane 7, CD-MPRHis; lane 8, Dom9His. (B) Enzymatic deglycosylation of purified wild-type Dom5His (lanes 1 and 2) and N711Q (lanes 3 and 4) was performed by incubating the protein with (lanes 2 and 4) or without (lanes 1 and 3) *endo* H for 16 h. The samples were resolved on a 12% nonreducing SDS−polyacrylamide gel and visualized by silver staining.

Expression and Purification of Truncated Forms of the CI-MPR and CD-MPR. We previously reported that *P. pastoris* yeast is a highly effective heterologous host system for the generation of functional, soluble forms of the bovine MPRs (*16*, *18*, *24*, *25*). In the current study, this system was used to generate truncated, soluble forms of the bovine CI-MPR composed of extracellular domain 5 alone (Dom5His) and domain 9 alone (Dom9His) and of the bovine CD-MPR (CD-MPRHis), each containing a C-terminal tag of six histidine residues to facilitate purification (Figure 2A). The constructs, which use the promoter from the glyceraldehyde 3-phosphate dehydrogenase gene for constitutive protein expression, are engineered in-frame with the 89-residue *Saccharomyces cerevisiae* α-factor signal sequence, resulting in proteins that are secreted from *P. pastoris*. The His-tagged proteins were purified from the culture medium by a single-step process using Ni−NTA chromatography. The purified CD-MPRHis contained a predominant glycosylated species that migrated with an apparent molecular mass of 19 kDa (Figure 3A, lane 7), whereas purified Dom9His contained both glycosylated (21 kDa) and nonglycosylated (17 kDa) forms (Figure 3A, lane 8, and data not shown). The Dom5His proteins migrated on SDS−polyacrylamide gels as multiple bands representing glycosylated and nonglycosylated forms (data not shown). To evaluate the role glycosylation plays in Man-6-P binding by domain 5, wild-type and mutant Dom5His proteins were subjected to additional affinity chromatography using ConA Sepharose. The proteins that were specifically eluted with methyl α-mannoside (i.e., glycosylated species) from ConA Sepharose were used in subsequent SPR analyses: wild-type Dom5His, Q644E, R687K, E709Q, and Y714F migrated as two major glycosylated species of 19 and 22 kDa (Figure 3A, lanes 1−5), whereas N711Q, which contains a single *N*-glycosylation site at position 591, migrates as a single species of 19 kDa (Figure 3A, lane 6). Enzymatic deglycosylation of Dom5His and N711Q with *endo* H resulted in a single 15 kDa protein, confirming that the 19 and 22 kDa species represent glycoforms of the receptor (Figure 3B).

Role of Gln-644, Arg-687, Glu-709, Tyr-714, and N-Glycosylation at Position 711 in Man-6-P Binding by Domain 5. SPR analyses were performed to determine the effect various single amino acid substitutions have on the binding of Dom5His to a lysosomal enzyme, β-glucuronidase. The overall structure of the mutants was evaluated by circular dichroism, and no significant differences between the spectra of the mutants and the wild-type protein were observed, indicating that the single amino acid substitutions resulted in no gross structural changes to the receptor (data not shown). Figure 4A shows that the affinity of the N711Q mutant for β-glucuronidase ($K_d = 99 \pm 12$ μM) does not differ significantly from that of wild-type Dom5His ($K_d = 91 \pm 5$ μM), demonstrating that the presence or absence of an oligosaccharide at position 711 does not influence the ability of Dom5His to interact with a lysosomal enzyme. In contrast, no detectable binding was observed by the Q644E, R687K, E709Q, and Y714F mutants (Figure 4A). These results are consistent with our prediction, as derived from the structure-based sequence alignment of domain 5 with the high-affinity Man-6-P binding sites of the CI-MPR (i.e., domains 1−3 and 9) and the CD-MPR (Figure 2B), that Gln-644, Arg-687, Glu-709, and Tyr-714 are essential residues for carbohydrate recognition by domain 5 of the CI-MPR.

Generation of GAA with Defined N-Glycans. Previously, we have used the lysosomal enzyme β-glucuronidase to determine the binding affinity of various mutant forms of the CD-MPR and CI-MPR (*17*, *24*, *32*). We chose human β-glucuronidase for our studies since it has been characterized extensively and its crystal structure has been determined (*33*). Human β-glucuronidase is heavily glycosylated, with each subunit of this homotetrameric enzyme containing four N-linked oligosaccharides, and only two out of the four *N*-glycans are preferentially phosphorylated (*34*). Therefore, as synthesized by mammalian cells, the oligosaccharides of human β-glucuronidase are heterogeneous. To probe the ligand specificity of the MPRs with molecules that are endogenous ligands for the receptors, a novel approach was taken to generate lysosomal enzymes with *N*-glycans that are defined in their phosphomannosyl content.

GAA containing either phosphomonoester (GAA monoester) or phosphodiester (GAA diester) moieties was generated from recombinant human GAA by in vitro enzymatic reactions. GAA contains seven *N*-glycosylation sites at positions 140, 233, 390, 470, 652, 882, and 925 (*35*) that are all efficiently glycosylated, except Asn-925, which exhibits only ~50% occupancy (internal communication, Genzyme Corp.). Carbohydrate composition analysis demonstrated that the glycans on recombinant human GAA isolated from the medium of CHO-K1 cells cultured in the presence of the α-mannosidase inhibitor kifunensine were exclusively of the high-mannose type (this GAA is referred to as HM-GAA), with 8.35 mannose residues on average

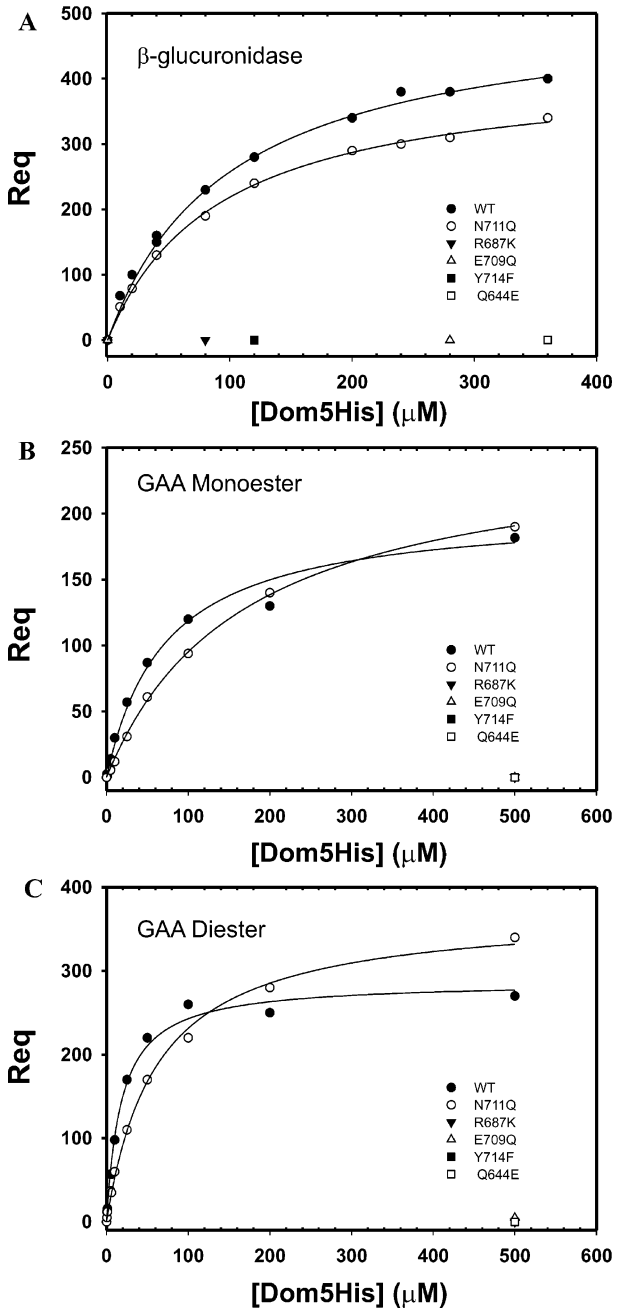

FIGURE 4: Interaction of Dom5His constructs with lysosomal enzymes. SPR analysis of Dom5His constructs binding to immobilized β-glucuronidase (A), immobilized GAA phosphomonoester (B), or immobilized GAA phosphodiester (C). β-glucuronidase, GAA monoester, and GAA diester were immobilized on the surface of a CM5 sensor chip to a level of 2500, 2500, and 1600 RU, respectively. MPR constructs were injected in a volume of 80 μL over the sensor surface at a rate of 40 μL/min. After 2 min, the solutions containing the MPRs were replaced with buffer, and the complexes were allowed to dissociate for 2 min. R_{eq} was plotted against the concentration of the Dom5His construct. Various concentrations of the wild-type Dom5His and N711Q proteins (10, 20, 40, 80, 120, 200, 240, 280, and 360 μM) were injected over immobilized β-glucuronidase (A). Only the response obtained at the highest concentration of the mutants Q644E (360 μM), R687K (80 μM), E709Q (280 μM), and Y714F (120 μM) is shown in panel A. Various concentrations of the wild-type Dom5His and N711Q proteins (1, 5, 10, 25, 50, 100, 200, and 500 μM) were injected over immobilized GAA phosphomonoester (B), or immobilized GAA phosphodiester (C). Only the response obtained at the highest concentration (500 μM) of the mutants Q644E, R687K, E709Q, and Y714F is shown in panels B and C.

per oligosaccharide. In addition, the analysis demonstrated the presence of 1.6 mol of Man-6-P/mol of GAA, or 0.25 mol of Man-6-P/mol of glycan, which existed exclusively as a phosphomonoester (see Figure 1D) as assessed by separation of the released glycans by charge (Figure 5A).

The GAA precursor was generated by enzymatic transfer of GlcNAc-phosphate to HM-GAA by GlcNAc-phosphotransferase (Figure 1A, step 1; Figure 1D), an enzyme that has the ability to transfer one or two GlcNAc-phosphate groups onto a high-mannose-type glycan (*36*). The GAA diester and GAA monoester were generated from the GAA precursor (Figure 1D) by removal of endogenous monoester by spPAP and by removal of covering GlcNAc using the uncovering enzyme (Figure 1B, step 2), respectively. Carbohydrate composition analysis of GAA monoester demonstrated that 5.5 mol of GlcNAc-phosphate was transferred to HM-GAA in addition to the 1.6 mol of naturally existing Man-6-P. Therefore, 1 mol of GAA precursor contains 5.5 mol of diester and 1.6 mol of monoester, and 1 mol each of GAA diester and GAA monoester contain 5.5 mol of diester and 7.1 mol of monoester, respectively. Separation by charge of released glycans derived from the GAA precursor (Figure 5B) and the GAA monoester (Figure 5C) demonstrated that the glycans were a mixture of neutral, monophosphorylated, and bisphosphorylated glycans. GAA diester and GAA monoester were used as MPR ligands with defined *N*-glycans in the following analyses.

SPR analyses of the various Dom5His constructs were repeated in which the GAA monoester and the GAA diester were immobilized on separate flow cells. Results similar to those observed with β-glucuronidase (Figure 4A) were obtained: the wild-type Dom5His and N711Q mutant bound with similar affinities to the GAA monoester coupled surface (WT, $K_d = 72 \pm 11$ μM; N711Q, $K_d = 170 \pm 7$ μM) and to the GAA diester coupled surface (WT, $K_d = 18 \pm 2$ μM; N711Q, $K_d = 61 \pm 4$ μM), whereas no detectable binding was observed for the Q644E, R687K, E709Q, and Y714F mutants to either GAA monoester (Figure 4B) or GAA diester (Figure 4C). These results further confirm the importance of Gln-644, Arg-687, Glu-709, and Tyr-714 in phosphomannosyl recognition by domain 5 of the CI-MPR. Furthermore, the results provide additional support for the lack of involvement of an oligosaccharide at position 711 in carbohydrate recognition by domain 5.

Domain 5, Unlike Domain 9 or the CD-MPR, Binds with Higher Affinity to Man-P-GlcNAc than Man-6-P. Surprisingly, our initial analysis of the interaction of Dom5His with the two different GAA glycoforms showed that domain 5 binds with a 4-fold higher affinity to the GAA diester ($K_d = 18 \pm 2$ μM, Figure 4C) than to the GAA monoester ($K_d = 72 \pm 11$ μM, Figure 4B). This is in contrast to the CD-MPR and domain 9 of the CI-MPR, which previously have been shown to interact with low affinity to a methyl diester (Man-6-POCH$_3$) present on *Dictyostelium discoideum*, but not mammalian, lysosomal enzymes (*19*, *37*). However, the binding affinity of the CD-MPR or the CI-MPR to a mammalian lysosomal enzyme containing the naturally occurring GlcNAc phosphodiester has not been determined. SPR analyses were carried out in which similar amounts of GAA monoester and GAA diester were immobilized to separate flow cells and increasing concentrations of Dom5His, CD-MPRHis, or Dom9His were passed over the sensor

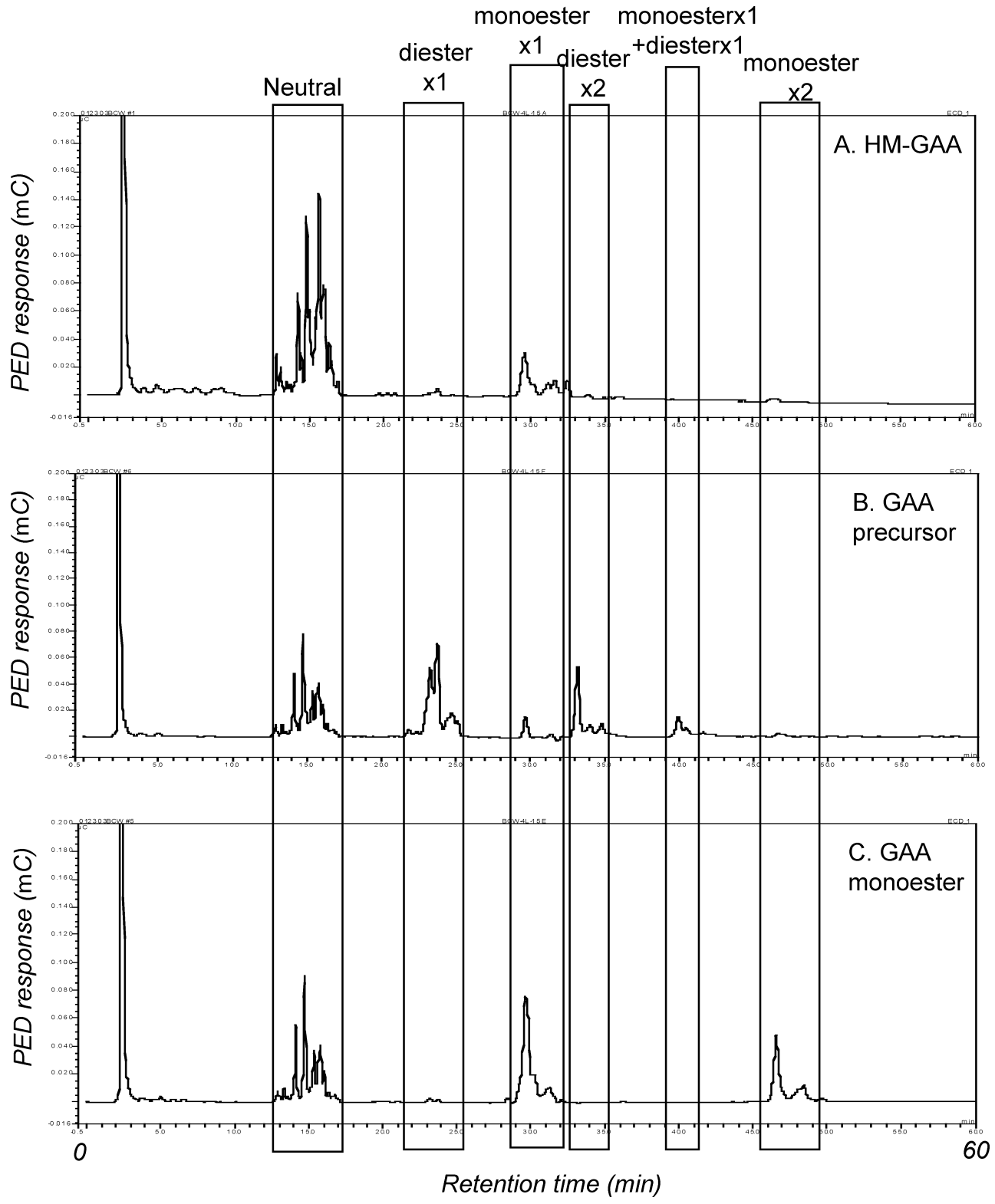

FIGURE 5: Charge separation of GAA glycans. High-mannose-type glycans on GAA molecules (A, HM-GAA; B, GAA precursor; C, GAA monoester) were released by PNGase F and separated by HPAEC on the basis of negative charge. Glycans with different numbers of phosphomonoester and/or phosphodiester moieties are indicated by boxes. The range of retention time for neutral high-mannose-type glycans (neutral) was determined using high-mannose-type glycan standards. Retention times for the glycans with one or two phosphodiesters (diester × 1 or diester × 2, respectively) were determined using glycans released from in vitro phosphorylated, but not uncovered, glycoproteins. Retention times for the glycans with one or two phosphomonoesters (monoester × 1 or monoester × 2, respectively) were determined using glycans released from in vitro phosphorylated and uncovered glycoproteins. The retention time for glycans with one phosphomonoester and one phosphodiester (monoester × 1 + diester × 1) was marked as in the figure since the signal disappeared after uncovering. (A) In addition to neutral glycans, HM-GAA contains a small population of endogenously phosphorylated glycans containing one phosphomonoester. (B) Glycans with one or two phosphodiesters were generated by incubation with GlcNAc-phosphotransferase. Thus, the GAA precursor contains phosphodiesters plus endogenous phosphomonoesters. (C) Removal of the GlcNAc moiety in phosphodiesters by the uncovering enzyme generated glycans with one or two phosphomonoesters and no detectable phosphodiester.

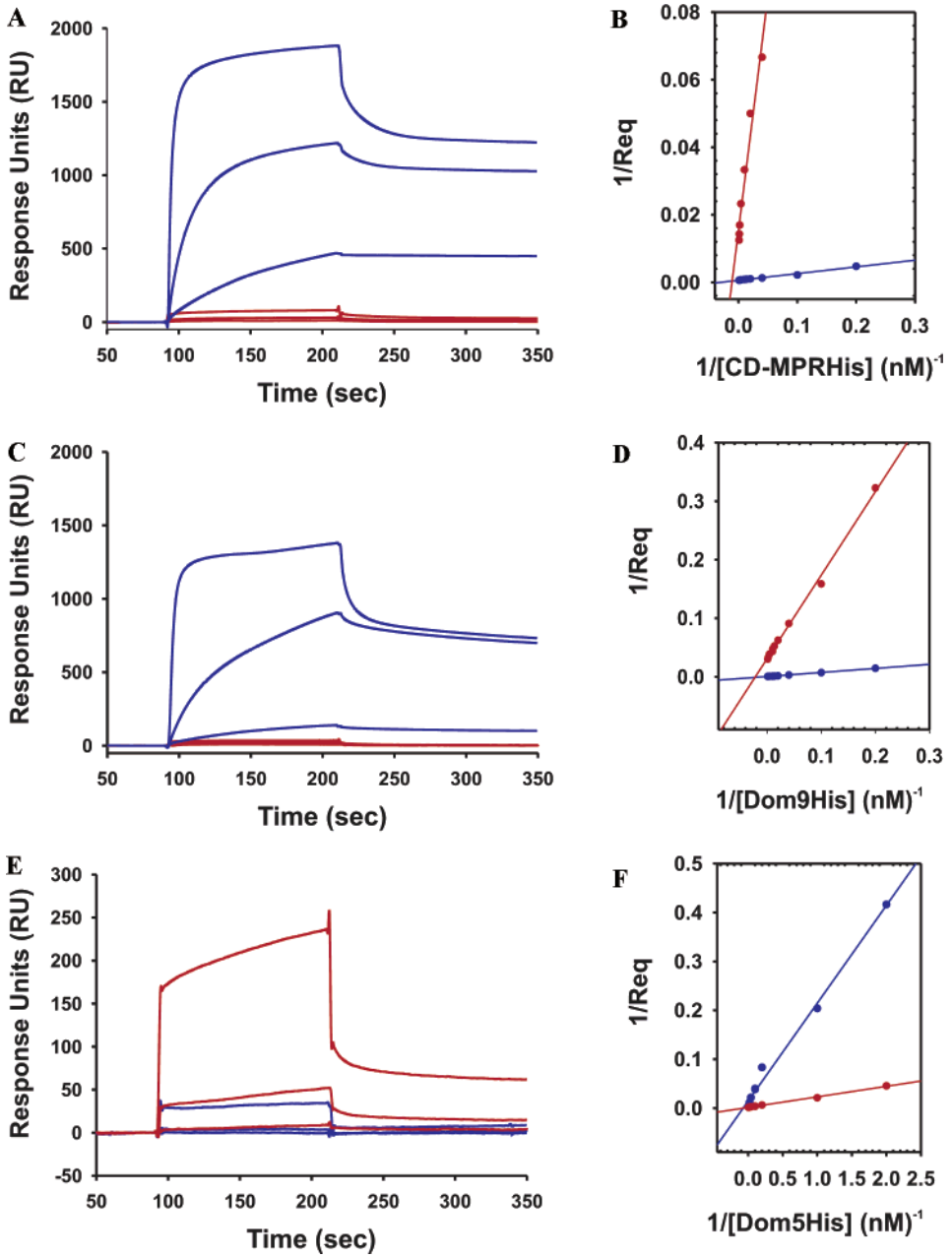

FIGURE 6: SPR analysis of MPR constructs binding to immobilized GAA phosphomonoester or GAA phosphodiester. Similar amounts (2500 and 2300 RU, respectively) of GAA monoester and GAA diester were immobilized on the surface of a CM5 sensor chip. MPR constructs were injected in a volume of 80 μL over the GAA and reference flow cells at a rate of 40 μL/min. After 2 min, the solutions containing the MPRs were replaced with buffer, and the complexes were allowed to dissociate for 2 min. Shown are representative sensorgrams for (A) CD-MPRHis at 10 nM, 100 nM, and 1 μM, (C) Dom9His at 10 nM, 100 nM, and 1 μM, and (E) Dom5His at 120 nM, 1 μM, and 10 μM comparing the response on GAA phosphomonoester (blue lines) and GAA phosphodiester (red lines) surfaces. An average of the R_{eq} values was determined for each MPR concentration using BIAevaluation version 4.0.1 software. The reciprocal plots (y intercept = $1/R_{max}$; x intercept = $-1/K_d$; slope = K_d/R_{max}) compare the R_{eq} for (B) CD-MPRHis at concentrations of 25, 50, 100, 250, 500, 750, and 1000 nM, (D) Dom9His at concentrations of 5, 10, 25, 50, 100, 250, 500, 750, and 1000 nM, and (F) Dom5His at concentrations of 0.5, 1, 5, 10, 25, 50, 100, and 200 μM on the GAA phosphomonoester (blue lines) and GAA phosphodiester (red lines) surfaces. Equilibrium constants were calculated from separate equilibrium binding curves (not shown) using nonlinear regression (SigmaPlot version 10.0) and are summarized in Table 1.

surface. The representative sensorgrams (Figure 6A,C,E) and corresponding reciprocal plots (Figure 6B,D,F) show strikingly that CD-MPRHis (Figure 6A,B) and Dom9His (Figure 6C,D) exhibit significant responses to the GAA monoester surface and minimal responses to the GAA diester surface whereas, in contrast, Dom5His displays significant interaction with the GAA diester surface and diminished binding to the GAA monoester surface (Figure 6E,F). The data were analyzed by nonlinear regression, and the affinity constants are summarized in Table 1. The affinity of Dom5His for the GAA diester (K_d = 18 ± 2 μM) is identical to that obtained from a sensor surface coupled with a lower density of GAA diester (i.e., 1600 RU (response units) (Figure 4C) versus 2300 RU (Figure 6)) and is ~24-fold higher than that observed for the GAA monoester (Table 1). In addition, SPR analyses of Dom5His, Dom9His, and CD-MPRHis were performed at different pH values (i.e., pH 5.5, 6.5, and 7.5). No significant differences were observed in the affinity of

Table 1: Summary of Affinity Constants and Maximal Responses for the Interaction of MPR Constructs with GAA Monoester and GAA Diester[a]

	monoester surface		diester surface	
construct	K_d (μM)	R_{max} (RU)	K_d (μM)	R_{max} (RU)
CD-MPRN81-His	0.032 ± 0.003	1640 ± 37	0.21 ± 0.05	90 ± 8.0
Dom9His	0.075 ± 0.011	1590 ± 77	0.046 ± 0.005	35 ± 1.0
Dom5His	438 ± 63	861 ± 92	18 ± 2.0	702 ± 18

[a] Equilibrium responses from Figure 6 were plotted versus the concentration of MPR. Equilibrium constants (K_d) and maximal responses (R_{max}) were calculated using nonlinear regression (SigmaPlot version 10.0).

the interaction between these three different receptors and either the GAA monoester or GAA diester, demonstrating that changes in pH did not alter the preference of the receptor for the phosphomonoester versus the GlcNA phosphodiester (data not shown).

The limited interaction of CD-MPRHis and Dom9His with the GAA diester surface is consistent with previous reports (*19*, *37*) (and Dahms's unpublished data) that these carbohydrate recognition sites bind a methyl diester (Man-6-$POCH_3$) with ~70-fold and ~250-fold lower affinity, respectively, than Man-6-P. However, in this study the determined affinity constants for CD-MPRHis and Dom9His are surprisingly similar for the GAA monoester when compared to the GAA diester (Table 1). Since the overall response (R_{max}) of CD-MPRHis and Dom9His to the GAA diester sensor surface is very low (Table 1), we took into consideration that the GAA diester contains small amounts of Man-6-P monoester. To test this hypothesis, the GAA precursor was subjected to SPR analysis. The results show that the response level of the precursor is intermediate between that of the GAA diester and GAA monoester while the affinity is similar to that of the GAA monoester (Supporting Information Figure 1). These results are consistent with low levels of monoester present in the GAA diester to account for the high-affinity interaction, but low response, observed with CD-MPRHis and Dom9His.

To further evaluate the interaction of individual binding sites of the CI-MPR with a lysosomal enzyme containing defined glycans, similar amounts of Dom5His and Dom9His were immobilized to separate flow cells on a CM5 sensor chip and increasing concentrations of GAA monoester and GAA diester were flowed over the sensor surface. Consistent with the above studies (Figure 6), Dom9His was specific for GAA containing phosphomonoesters ($K_d = 95 \pm 12$ nM), with little interaction observed with the GAA diester ($K_d = 1.4 \pm 1$ μM) (Figure 7A), while Dom5His bound specifically to the GAA diester surface ($K_d = 0.72 \pm 0.15$ μM) and no dectectable binding was observed to the GAA monoester surface (Figure 7B). Although it is unclear why the measured affinity of Dom5His to the GAA diester differed by 25-fold from that of the previous experiments in which the GAA diester, rather than Dom5His, was coupled to the sensor chip ($K_d = 18$ μM; see Figures 4C and 6E,F), the consistent finding in all of these studies is the ability of domain 5 to bind preferentially to GlcNAc phosphodiesters.

To directly measure the binding affinity of Dom5His to Man-6-P and Man-P-GlcNAc, Dom5His was passed over the sensor surface containing immobilized GAA monoester or GAA diester in the presence of increasing concentrations of Man-6-P, GlcNAc-P-methyl mannoside, or Glc-6-P. Glc-6-P was chosen as a control since it had been shown

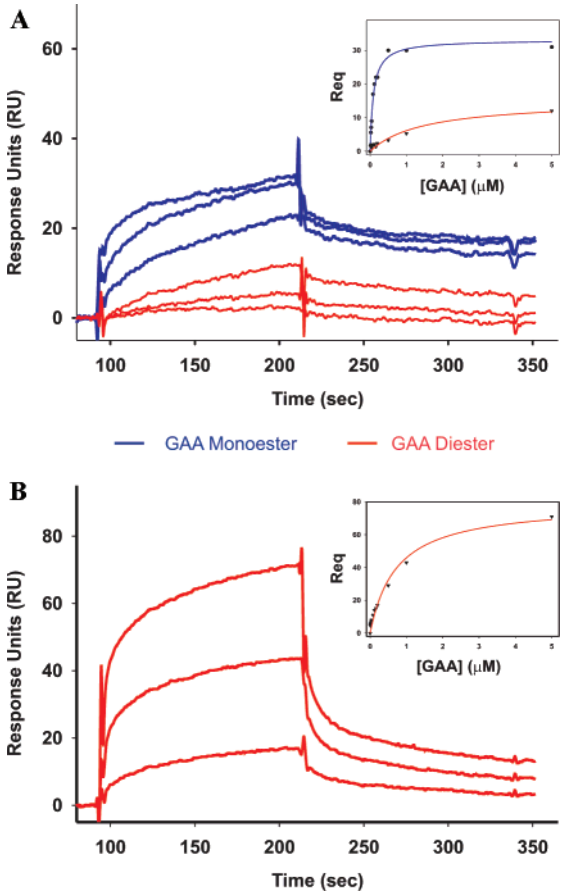

FIGURE 7: SPR analysis of GAA phosphomonoester and GAA phosphodiester binding to immobilized Dom9His or Dom5His. Similar amounts (1200 and 1100 RU, respectively) of Dom9His (A) and Dom5His (B) were immobilized to separate flow cells of a CM5 sensor chip, and various concentrations (7.5, 10, 15, 20, 30, 40, 80, 120, 160, 200, 500, 1000, and 5000 nM) of GAA phosphomonoester or GAA phosphodiester were injected in a volume of 80 μL over the receptor and reference flow cells at a rate of 40 μL/min. After 2 min, the solutions containing GAA were replaced with buffer, and the complexes were allowed to dissociate for 2 min. Shown are representative sensorgrams at 200, 1000, and 5000 nM GAA phosphomonoester (blue) or GAA phosphodiester (red). The inset shows R_{eq} plotted against the concentration of GAA phosphomonoester (blue) or GAA phosphodiester (red).

previously to bind with low affinity ($K_d = (1-8 \times 10^{-2}$ M) to the CD-MPR and CI-MPR (*14*). The results demonstrate that Dom5His binds with 14−18-fold higher affinity to Man-P-GlcNAc ($K_i = 1$ mM) than to Man-6-P ($K_i = 14-18$ mM), with inhibition by Glc-6-P being observed only at high concentrations (i.e., above 10 mM) (Figure 8A,B). In contrast, Man-P-GlcNAc, like Glc-6-P, did not inhibit the interaction of Dom9His with GAA at concentrations up to 5 mM (Figure 8C,D). Taken together, these results demonstrate that, unlike the CD-MPR and domain 9, domain 5 of

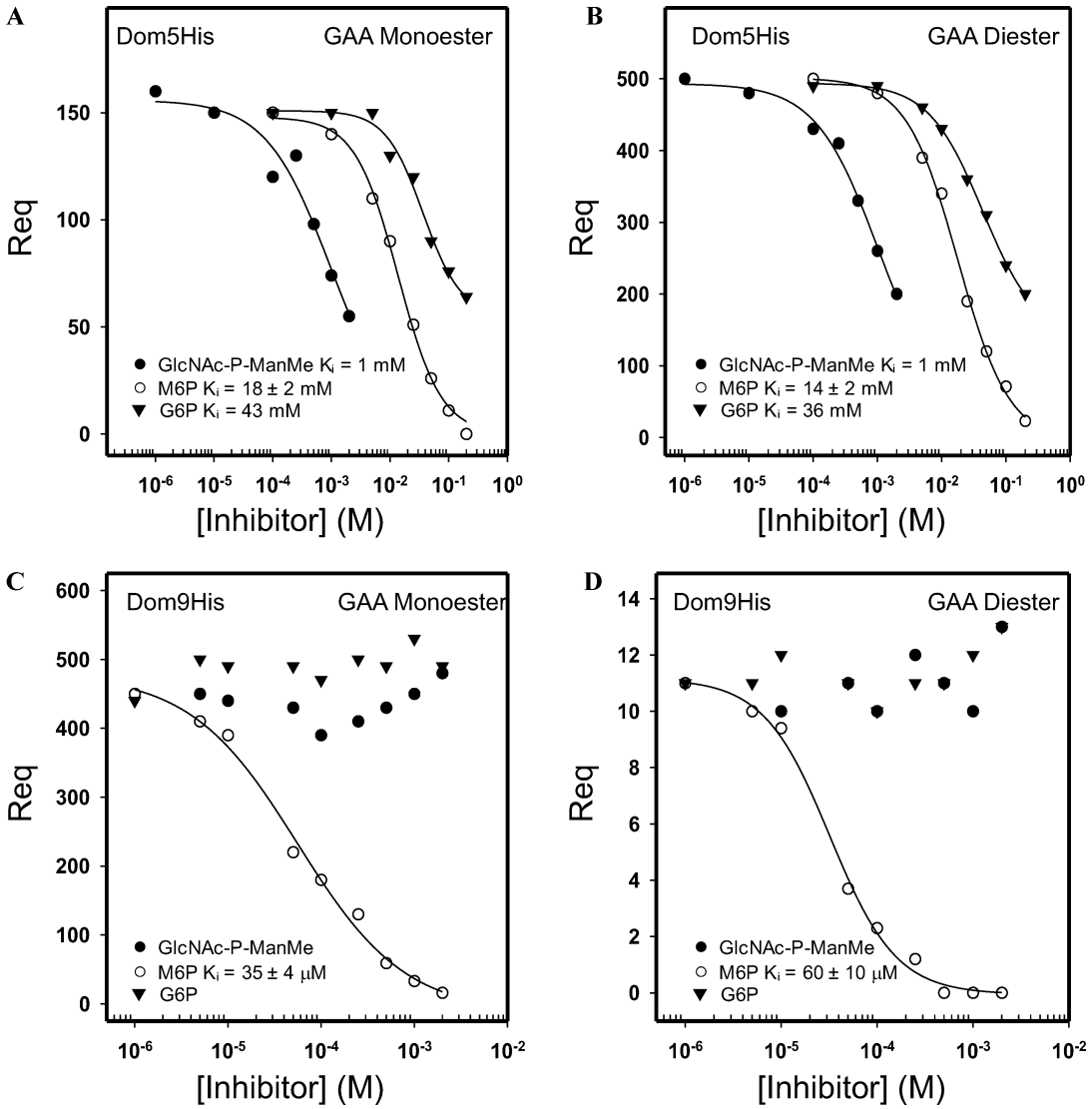

FIGURE 8: Inhibition of MPR binding to GAA by Man-6-P, Glc-6-P, and *N*-acetylglucosaminyl 6-phosphomethylmannoside diester. Aliquots of 500 nM Dom5His (A, B) and 50 nM Dom9His (C, D) were incubated with increasing concentrations of Glc-6-P (▼), Man-6-P (○), or *N*-acetylglucosaminyl 6-phosphomethylmannoside diester (●) and injected over a flow cell coupled with GAA monoester (A, C) or GAA diester (B, D). Similar amounts (3300 and 2800 RU, respectively) of GAA monoester and GAA diester were immobilized on the surface of a CM5 sensor chip. R_{eq} from the resulting sensorgrams was plotted against the log of the inhibitor concentration. K_i was determined using nonlinear regression (SigmaPlot, version 10.0).

the CI-MPR binds preferentially to lysosomal enzymes containing phosphodiesters (Man-P-GlcNAc).

DISCUSSION

The MPRs constitute a highly specific recognition and delivery system by carrying phosphomannosyl-containing proteins (e.g., soluble lysosomal enzymes) from the biosynthetic pathway or the cell surface to endosomal compartments (*1*−*3*). The importance of this targeting process in the generation of lysosomes containing a full complement of hydrolytic enzymes is evidenced by the existence of over 40 different lysosomal storage disorders, the majority of which are caused by a deficiency of a single lysosomal enzyme that results in the accumulation or storage of undigested endogenous macromolecules within lysosomes (*38*−*40*). Enzyme replacement therapy, in which the missing enzyme is supplied to the patient by intravenous injection on a weekly basis, has been shown to partially or completely reverse lysosomal storage in many target tissues. To date, three (Fabry disease, mucopolysaccharidosis I, and Pompe disease) out of the four Food and Drug Administration approved enzyme replacement therapies target the MPRs for the uptake of the infused Man-6-P-containing enzyme (*41*). In addition to lysosomal enzymes, the repertoire of identified extracellular ligands of the CI-MPR has expanded to include a diverse spectrum of Man-6-P-containing proteins (*42*). For example, varicella-zoster virus expresses Man-6-P-containing viral glycoproteins which function to facilitate the entry of the virus into mammalian cells via the CI-MPR (*43*, *44*), while the transforming growth factor-β precursor becomes activated following its interaction with the CI-MPR (*45*). This list continues to expand as recent proteomic approaches using affinity columns containing immobilized CI-MPR have identified new Man-6-P-containing proteins (*46*, *47*). Thus, an understanding of the molecular basis by which MPRs recognize a diversity of targets may lead to the development of new and improved therapies for the treatment of lysosomal storage disorders and other human diseases. In the current

study, the structural elements of domain 5 of the CI-MPR which are important for carbohydrate recognition were identified. In addition, the generation of lysosomal enzymes with defined *N*-glycans containing either phosphomonoesters or GlcNAc phosphodiesters provided unique tools to further characterize the binding properties of the CD-MPR and CI-MPR.

Previous equilibrium dialysis studies demonstrated that the CI-MPR contains two high-affinity Man-6-P binding sites (*15*) that have been mapped to discrete regions (domains 1−3 and 9) within its extracellular region (*16*, *48*). The crystal structure of the extracytoplasmic region of the CD-MPR (*20*, *21*) and the N-terminal Man-6-P binding site of the CI-MPR (*22*) in the presence of bound Man-6-P identified those residues within hydrogen-bonding distance to this phosphorylated sugar, revealing five residues (corresponding to Tyr-45, Gln-66, Arg-111, Glu-133, and Tyr-143 of the CD-MPR) that are conserved between the binding pockets of the two receptors. A structure-based sequence alignment demonstrated that these residues are also conserved in domain 9, the other known high-affinity Man-6-P binding site, and in domain 5 of the CI-MPR (see Figure 2B), leading to the speculation that domain 5 contains a carbohydrate binding site (*18*). This hypothesis was confirmed by oligosaccharide microarray and pentamannosyl phosphate−agarose affinity chromatography analyses (*18*). Previous mutagenesis studies demonstrated that four of these residues (corresponding to Gln-66, Arg-111, Glu-133, and Tyr-143 of the CD-MPR) are essential for Man-6-P binding as substitution of any one of these residues resulted in a ~1000-fold decrease in binding affinity by the CD-MPR (*24*) and domains 3 and 9 of the CI-MPR (*17*). In the current study, these conserved residues (Gln-644, Arg-687, Glu-709, and Tyr-714) were also found to be critical for Man-6-P binding by domain 5 of the CI-MPR (Figure 4). Thus, all of the Man-6-P binding sites of the two MPRs share a common feature: four residues (Gln, Arg, Glu, Tyr), which are positionally conserved in the linear amino acid sequence (Figure 2B) and have been shown from the crystal structure of the CD-MPR (*20*, *21*) and domains 1−3 of the CI-MPR (*22*) to be located in identical positions in the binding pocket and contact the 2-, 3-, and 4- hydroxyl groups of the mannose ring, are critical determinants for carbohydrate recognition by the MPRs. Taken together, these results suggest that the carbohydrate binding sites of the MPRs arose from a common ancestor, utilizing the same protein fold and identical residues to bind the mannose ring. It is interesting to note that the binding pocket architecture surrounding the phosphate group of Man-6-P has not been conserved: the CD-MPR (*20*, *21*) uses Asp-103, Asn-104, and His-105, whereas domain 3 of the CI-MPR (*22*) uses Ser-386 and an ordered water molecule to coordinate the phosphate group of Man-6-P. The structure-based sequence alignment indicates different residues may be involved in phosphate recognition by domains 5 and 9 of the CI-MPR (Figure 2B). Clearly, the three-dimensional structure of domains 5 and 9 of the CI-MPR will be needed to determine whether these regions of the receptor have a fold and mechanism of Man-6-P binding similar to those of the CD-MPR and domain 3 of the CI-MPR.

In contrast to the nanomolar affinities observed by domains 1−3 and 9 of the CI-MPR for the lysosomal enzyme β-glucuronidase (*16*), domain 5 bound the lysosomal enzyme with a much lower affinity ($K_d = 91 \pm 5$ μM) (Figure 4A). The observation that domain 5 is missing two cysteines (Figure 2B) that form a critical disulfide bridge within the binding pocket of the CD-MPR (*20*, *21*) and domain 3 of the CI-MPR (*22*) may provide an explanation for the lower binding affinity exhibited by domain 5. In place of one of these cysteine residues is a serine residue that comprises an *N*-glycosylation site at position 711. To test the possibility that the presence of an *N*-glycan could affect the ligand binding ability of domain 5, the aspargine residue at position 711 was replaced with a glutamine residue and the mutant was assayed by SPR for its ability to bind β-glucuronidase, GAA monoester, and GAA diester. No significant difference in binding affinity was detected (Figure 4), demonstrating that the presence or absence of an *N*-glycan at this position has little influence on the ability of domain 5 to bind a lysosomal enzyme.

A surprising finding of the current study is the observation that domain 5 of the CI-MPR binds GlcNAc phosphodiesters with a higher affinity than phosphomonoesters (Figures 4 and 6−8). Binding inhibition studies demonstrated that this preference is on the order of 14−18-fold (Figure 8). This is in sharp contrast to that observed for the other carbohydrate binding sites of the MPRs that exhibit a strong preference for Man-6-P. Previously, the ability of the MPRs to recognize phosphodiesters was probed with lysosomal enzymes derived from *Dictyostelium discoideum* which contain the smaller methyl phosphodiester, Man-6-P-OCH_3, a modification not found on mammalian lyososomal enzymes (*49*). Early studies using full-length CD-MPR and CI-MPR showed that the CI-MPR (*15*), but not the CD-MPR (*37*), bound *D. discoideum* lysosomal enzymes. However, these results are difficult to assess since *D. discoideum* lysosomal enzymes also contain mannose 6-sulfate (*50*). Binding experiments using Man-6-P and Man-6-P-OCH_3 as inhibitors of the individual high-affinity Man-6-P binding sites of the CI-MPR clarified these earlier studies and demonstrated that constructs containing domain 9 were highly specific for the phosphomonoester and bound Man-6-P with a ~250-fold higher affinity than Man-6-P-OCH_3, whereas domains 1−3 also preferred Man-6-P, binding Man-6-P with a ~10-fold higher affinity than Man-6-P-OCH_3 (*16*, *19*). Inhibition studies using GlcNAc-P-ManMe confirmed the high degree of specificity for the phosphomonoester Man-6-P and no detectable inhibition of binding of domain 9 was observed with GlcNAc-P-ManMe up to concentrations of 5 mM (Figure 8). Previous qualitative studies in which oligosaccharides containing two GlcNAc phosphodiesters were passed over a column containing immobilized CI-MPR showed no significant interaction with the receptor (*36*). However, a subsequent study in which equilibrium dialysis was used to evaluate the interaction of [^{3}H]GlcNAc-α-P-Man-α-Me with the CI-MPR estimated an affinity that was ~15-fold lower than that observed with [^{3}H]-Man-6-P (*15*), a finding consistent with our inhibition binding studies using domain 5 of the CI-MPR (Figure 8). Thus, our studies extend these early reports by demonstrating that lysosomal enzymes bearing GlcNAc phosphodiesters can interact with the CI-MPR, but not the CD-MPR. Furthermore, the current studies have identified the region of the CI-MPR (i.e., domain 5) that is responsible for this activity. In addition, the ability of domain 5 to interact with a GlcNAc phosphodiester suggests that the architecture of its binding

pocket surrounding the phosphate moiety must be significantly different from that of the other Man-6-P binding sites to accommodate and form specific contacts with the GlcNAc sugar. It is interesting to speculate that the absence of the two cysteine residues in domain 5, which forms an essential tether of loops in the binding pocket of the CD-MPR (*20*, *21*) and domain 3 of the CI-MPR (*22*), may allow for a more open binding pocket in domain 5 to accommodate a GlcNAc phosphodiester.

Although the ability of the CI-MPR via domain 5 to interact with GlcNAc phosphodiesters in the context of a lysosomal enzyme has been clearly demonstrated, the impact of this interaction in the functioning of the CI-MPR remains to be clarified. One possible role involves the targeting of newly synthesized lysosomal enzymes that are not efficiently modified by the uncovering enzyme in the TGN, resulting in the retention of GlcNAc phosphodiesters on a subset of lysosomal enzymes. To date, a genetic disease attributable to a deficiency of the uncovering enzyme has not been described. This could be due to the ability of the CI-MPR to rescue the phenotype by targeting GlcNAc-covered enzymes to the lysosome. Another possibility relates to a report that the CI-MPR interacts with GPI-linked molecules, which is dependent upon a Man-6-P diester rather than the inositol 1,2-cyclic phosphate group (*51*). This interaction with the CI-MPR was speculated to influence the clustering and subsequent transmembrane signaling of GPI-linked molecules (*51*). The GPI portion of mammalian GPI-linked proteins is quite variable and contains several types of diesters including Man-6-P-GlcNAc (*52*) and mannose 2-phosphate diesters (*53*). Thus, it is possible that phosphodiesters other than Man-6-P-GlcNAc may serve as high-affinity ligands for domain 5. It is also possible that non-phosphate-containing glycans may be the preferred ligand for this region of the receptor. Therefore, additional studies will be required to probe whether other endogenous molecules exist that interact with high affinity to domain 5 of the CI-MPR. Future studies will focus on testing these intriguing possibilities and determining the three-dimensional structure of domain 5.

ACKNOWLEDGMENT

We thank Dr. Linda Olson for providing Dom9His protein, Dr. Guangjie Sun for performing the SPR analyses of the interaction between Dom5His and β-glucuronidase, and Dr. Jung-Ja Kim for critical reading of the manuscript.

SUPPORTING INFORMATION AVAILABLE

Figure showing that the response level of the precursor is intermediate between that of the GAA diester and GAA monoester while the affinity is similar to that of the GAA monoester. This material is available free of charge via the Internet at http://pubs.acs.org.

REFERENCES

1. Ghosh, P., Dahms, N. M., and Kornfeld, S. (2003) Mannose 6-phosphate receptors: new twists in the tale, *Nat. Rev. Mol. Cell Biol. 4*, 202−213.
2. Mullins, C., and Bonifacino, J. S. (2001) The molecular machinery for lysosome biogenesis, *Bioessays 23*, 333−343.
3. Dell'Angelica, E. C., and Payne, G. S. (2001) Intracellular cycling of lysosomal enzyme receptors. cytoplasmic tails' tales, *Cell 106*, 395−398.
4. Hasilik, A., Klein, U., Waheed, A., Strecker, G., and von Figura, K. (1980) Phosphorylated oligosaccharides in lysosomal enzymes: identification of alpha-N-acetylglucosamine(1)phospho-(6)mannose diester groups, *Proc. Natl. Acad. Sci. U.S.A. 77*, 7074−7078.
5. Varki, A., and Kornfeld, S. (1980) Structural studies of phosphorylated high mannose-type oligosaccharides, *J. Biol. Chem. 255*, 10847−10858.
6. Bao, M., Booth, J. L., Elmendorf, B. J., and Canfield, W. M. (1996) Bovine UDP-N-acetylglucosamine:lysosomal-enzyme N-acetylglucosamine-1-phosphotransferase. I. Purification and subunit structure, *J. Biol. Chem. 271*, 31437−31445.
7. Kudo, M., Bao, M., D'Souza, A., Ying, F., Pan, H., Roe, B. A., and Canfield, W. M. (2005) The alpha- and beta-subunits of the human UDP-N-acetylglucosamine:lysosomal enzyme phosphotransferase are encoded by a single cDNA, *J. Biol. Chem. 280*, 36141−36149.
8. Kornfeld, R., Bao, M., Brewer, K., Noll, C., and Canfield, W. (1999) Molecular cloning and functional expression of two splice forms of human N-acetylglucosamine-1-phosphodiester alpha-N-acetylglucosaminidase, *J. Biol. Chem. 274*, 32778−32785.
9. Do, H., Lee, W. S., Ghosh, P., Hollowell, T., Canfield, W., and Kornfeld, S. (2002) Human mannose 6-phosphate-uncovering enzyme is synthesized as a proenzyme that is activated by the endoprotease furin, *J. Biol. Chem. 277*, 29737−29744.
10. Varki, A., Sherman, W., and Kornfeld, S. (1983) Demonstration of the enzymatic mechanisms of alpha-N-acetyl-D-glucosamine-1-phosphodiester N-acetylglucosaminidase (formerly called alpha-N-acetylglucosaminylphosphodiesterase) and lysosomal alpha-N-acetylglucosaminidase, *Arch. Biochem. Biophys. 222*, 145−149.
11. Waheed, A., Hasilik, A., and von Figura, K. (1981) Processing of the phosphorylated recognition marker in lysosomal enzymes. Characterization and partial purification of a microsomal alpha-N-acetylglucosaminyl phosphodiesterase, *J. Biol. Chem. 256*, 5717−5721.
12. Rohrer, J., and Kornfeld, R. (2001) Lysosomal hydrolase mannose 6-phosphate uncovering enzyme resides in the trans-Golgi network, *Mol. Biol. Cell 12*, 1623−1631.
13. Lobel, P., Dahms, N. M., and Kornfeld, S. (1988) Cloning and sequence analysis of the cation-independent mannose 6- phosphate receptor, *J. Biol. Chem. 263*, 2563−2570.
14. Tong, P. Y., and Kornfeld, S. (1989) Ligand interactions of the cation-dependent mannose 6-phosphate receptor. Comparison with the cation-independent mannose 6-phosphate receptor, *J. Biol. Chem. 264*, 7970−7975.
15. Tong, P. Y., Gregory, W., and Kornfeld, S. (1989) Ligand interactions of the cation-independent mannose 6-phosphate receptor. The stoichiometry of mannose 6-phosphate binding, *J. Biol. Chem. 264*, 7962−7969.
16. Hancock, M. K., Yammani, R. D., and Dahms, N. M. (2002) Localization of the carbohydrate recognition sites of the insulin-like growth factor II/mannose 6-phosphate receptor to domains 3 and 9 of the extracytoplasmic region, *J. Biol. Chem. 277*, 47205−47212.
17. Hancock, M. K., Haskins, D. J., Sun, G., and Dahms, N. M. (2002) Identification of residues essential for carbohydrate recognition by the insulin-like growth factor II/mannose 6-phosphate receptor, *J. Biol. Chem. 277*, 11255−11264.
18. Reddy, S. T., Chai, W., Childs, R. A., Page, J. D., Feizi, T., and Dahms, N. M. (2004) Identification of a low affinity mannose 6-phosphate-binding site in domain 5 of the cation-independent mannose 6-phosphate receptor, *J. Biol. Chem. 279*, 38658−38667.
19. Marron-Terada, P. G., Hancock, M. K., Haskins, D. J., and Dahms, N. M. (2000) Recognition of Dictyostelium discoideum lysosomal enzymes is conferred by the amino-terminal carbohydrate binding site of the insulin-like growth factor II/mannose 6-phosphate receptor, *Biochemistry 39*, 2243−2253.
20. Roberts, D. L., Weix, D. J., Dahms, N. M., and Kim, J.-J. P. (1998) Molecular basis of lysosomal enzyme recognition: three-dimensional structure of the cation-dependent mannose 6-phosphate receptor, *Cell 93*, 639−648.
21. Olson, L. J., Zhang, J., Lee, Y. C., Dahms, N. M., and Kim, J.-J. P. (1999) Structural basis for recognition of phosphorylated high mannose oligosaccharides by the cation-dependent mannose 6-phosphate receptor, *J. Biol. Chem. 274*, 29889−29896.
22. Olson, L. J., Dahms, N. M., and Kim, J. J. (2004) The N-terminal carbohydrate recognition site of the cation-independent mannose 6-phosphate receptor, *J. Biol. Chem. 279*, 34000−34009.

23. Olson, L. J., Hancock, M. K., Dix, D., Kim, J.-J. P., and Dahms, N. M. (1999) Mutational analysis of the binding site residues of the bovine cation-dependent mannose 6-phosphate receptor, *J. Biol. Chem. 274*, 36905−36911.
24. Sun, G., Zhao, H., Kalyanaraman, B., and Dahms, N. M. (2005) Identification of residues essential for carbohydrate recognition and cation dependence of the 46-kDa mannose 6-phosphate receptor, *Glycobiology 15*, 1136−1149.
25. Reddy, S. T., and Dahms, N. M. (2002) High-level expression and characterization of a secreted recombinant cation-dependent mannose 6-phosphate receptor in Pichia pastoris, *Protein Expression Purif. 26*, 290−300.
26. Marron-Terada, P. G., Brzycki-Wessell, M. A., and Dahms, N. M. (1998) The two mannose 6-phosphate binding sites of the insulin-like growth factor-II/mannose 6-phosphate receptor display different ligand binding properties, *J. Biol. Chem. 273*, 22358−22366.
27. Kudo, M., and Canfield, W. M. (2006) Structural requirements for efficient processing and activation of recombinant human UDP-N-acetylglucosamine:lysosomal-enzyme-N-acetylglucosamine-1-phosphotransferase, *J. Biol. Chem. 281*, 11761−11768.
28. Hefler, S. K., and Averill, B. A. (1987) The "manganese(III)-containing" purple acid phosphatase from sweet potatoes is an iron enzyme, *Biochem. Biophys. Res. Commun. 146*, 1173−1177.
29. Moreland, R. J., Jin, X., Zhang, X. K., Decker, R. W., Albee, K. L., Lee, K. L., Cauthron, R. D., Brewer, K., Edmunds, T., and Canfield, W. M. (2005) Lysosomal acid alpha-glucosidase consists of four different peptides processed from a single chain precursor, *J. Biol. Chem. 280*, 6780−6791.
30. Mullis, K. G., and Ketcham, C. M. (1992) The synthesis of substrates and two assays for the detection of N-acetylglucosamine-1-phosphodiester alpha-N-acetylglucosaminidase (uncovering enzyme), *Anal. Biochem. 205*, 200−207.
31. Myszka, D. G. (2000) Kinetic, equilibrium, and thermodynamic analysis of macromolecular interactions with BIACORE, *Methods Enzymol. 323*, 325−340.
32. Marron-Terada, P. G., Bollinger, K. E., and Dahms, N. M. (1998) Characterization of truncated and glycosylation-deficient forms of the cation-dependent mannose 6-phosphate receptor expressed in baculovirus- infected insect cells, *Biochemistry 37*, 17223−17229.
33. Jain, S., Drendel, W. B., Chen, Z. W., Mathews, F. S., Sly, W. S., and Grubb, J. H. (1996) Structure of human beta-glucuronidase reveals candidate lysosomal targeting and active-site motifs, *Nat. Struct. Biol. 3*, 375−381.
34. Shipley, J. M., Grubb, J. H., and Sly, W. S. (1993) The role of glycosylation and phosphorylation in the expression of active human beta-glucuronidase, *J. Biol. Chem. 268*, 12193−12198.
35. Martiniuk, F., Mehler, M., Tzall, S., Meredith, G., and Hirschhorn, R. (1990) Sequence of the cDNA and 5′-flanking region for human acid alpha-glucosidase, detection of an intron in the 5′ untranslated leader sequence, definition of 18-bp polymorphisms, and differences with previous cDNA and amino acid sequences, *DNA Cell Biol. 9*, 85−94.
36. Varki, A., and Kornfeld, S. (1983) The spectrum of anionic oligosaccharides released by endo-beta-N-acetylglucosaminidase H from glycoproteins. Structural studies and interactions with the phosphomannosyl receptor, *J. Biol. Chem. 258*, 2808−2818.
37. Distler, J. J., Guo, J. F., Jourdian, G. W., Srivastava, O. P., and Hindsgaul, O. (1991) The binding specificity of high and low molecular weight phosphomannosyl receptors from bovine testes. Inhibition studies with chemically synthesized 6-O-phosphorylated oligomannosides, *J. Biol. Chem. 266*, 21687−21692.
38. Neufeld, E. F. (1991) Lysosomal storage diseases, *Annu. Rev. Biochem. 60*, 257−280.
39. Vellodi, A. (2004) Lysosomal storage disorders, *Br. J Haematol. 128*, 413−431.
40. Futerman, A. H., and van Meer, G. (2004) The cell biology of lysosomal storage disorders, *Nat. Rev. Mol. Cell Biol. 5*, 554−565.
41. Brady, R. O. (2006) Enzyme replacement for lysosomal diseases, *Annu. Rev. Med. 57*, 283−296.
42. Dahms, N. M., and Hancock, M. K. (2002) P-type lectins, *Biochim. Biophys. Acta 1572*, 317−340.
43. Gabel, C. A., Dubey, L., Steinberg, S. P., Sherman, D., Gershon, M. D., and Gershon, A. A. (1989) Varicella-zoster virus glycoprotein oligosaccharides are phosphorylated during posttranslational maturation, *J. Virol. 63*, 4264−4276.
44. Chen, J. J., Zhu, Z., Gershon, A. A., and Gershon, M. D. (2004) Mannose 6-phosphate receptor dependence of varicella zoster virus infection in vitro and in the epidermis during varicella and zoster, *Cell 119*, 915−926.
45. Dennis, P. A., and Rifkin, D. B. (1991) Cellular activation of latent transforming growth factor beta requires binding to the cation-independent mannose 6-phosphate/insulin-like growth factor type II receptor, *Proc. Natl. Acad. Sci. U.S.A. 88*, 580−584.
46. Czupalla, C., Mansukoski, H., Riedl, T., Thiel, D., Krause, E., and Hoflack, B. (2006) Proteomic analysis of lysosomal acid hydrolases secreted by osteoclasts: implications for lytic enzyme transport and bone metabolism, *Mol. Cell. Proteomics 5*, 134−143.
47. Sleat, D. E., Wang, Y., Sohar, I., Lackland, H., Li, Y., Li, H., Zheng, H., and Lobel, P. (2006) Identification and validation of mannose 6-phosphate glycoproteins in human plasma reveal a wide range of lysosomal and non-lysosomal proteins, *Mol. Cell. Proteomics 5*, 1942−1956.
48. Westlund, B., Dahms, N. M., and Kornfeld, S. (1991) The bovine mannose 6-phosphate/insulin-like growth factor II receptor. Localization of mannose 6-phosphate binding sites to domains 1-3 and 7-11 of the extracytoplasmic region, *J. Biol. Chem. 266*, 23233−23239.
49. Gabel, C. A., Costello, C. E., Reinhold, V. N., Kurz, L., and Kornfeld, S. (1984) Identification of methylphosphomannosyl residues as components of the high mannose oligosaccharides of Dictyostelium discoideum glycoproteins, *J. Biol. Chem. 259*, 13762−13769.
50. Freeze, H. H., and Wolgast, D. (1986) Structural analysis of N-linked oligosaccharides from glycoproteins secreted by Dictyostelium discoideum. Identification of mannose 6-sulfate, *J. Biol. Chem. 261*, 127−134.
51. Green, P. J., Ferguson, M. A., Robinson, P. J., and Feizi, T. (1995) The cation-independent mannose-6-phosphate receptor binds to soluble GPI-linked proteins via mannose-6-phosphate, *FEBS Lett. 360*, 34−38.
52. Fukushima, K., Ikehara, Y., and Yamashita, K. (2005) Functional role played by the glycosylphosphatidylinositol anchor glycan of CD48 in interleukin-18-induced interferon-gamma production, *J. Biol. Chem. 280*, 18056−18062.
53. McConville, M. J., and Ferguson, M. A. (1993) The structure, biosynthesis and function of glycosylated phosphatidylinositols in the parasitic protozoa and higher eukaryotes, *Biochem. J. 294*, 305−324.

BI7011806